Impact of geological conceptualization in predicting pore pressure reduction from urban excavations

Engineering Geology 364 (2026) 108601

Contents lists available at ScienceDirect

Engineering Geology

journal homepage: www.elsevier.com/locate/enggeo

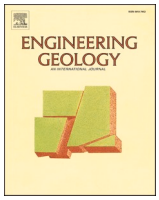

Impact of geological conceptualization in predicting pore pressure reduction from urban excavations

Sofie Axéen, Johanna Merisalu *, Ezra Haaf, Lars Rosén

Department of Architecture and Civil Engineering, Chalmers University of Technology, Sweden

ARTICLE INFO

Keywords:
Groundwater modelling
Conceptual model uncertainty
Sand lenses
Pore pressure reduction
MODFLOW
Multiple Point Statistics

ABSTRACT

Leakage of groundwater and subsequent pore pressure reduction can cause consolidation in subsidence sensitive soils and subsequently pose damage risks to the built environment. This study presents the first systematic, quantitative evaluation of how geological conceptualization – specifically the inclusion or exclusion of permeable sand lenses within glaciomarine clay deposits - affects simulated pore pressure reduction due to groundwater leakage into deep excavations. By employing Multiple Point Statistics (MPS) to generate alternative geological models and integrating these with MODFLOW-NWT transient groundwater simulations, we reveal that the presence and hydraulic connectivity of sand lenses significantly influence the rate and magnitude of pore pressure reduction in clay, which has significant consequences for settlement magnitudes. These findings underscore the importance of explicitly accounting for geological heterogeneity and uncertainty in risk assessment for urban excavations, a factor often neglected in conventional engineering geology practice when assessing settlement hazards and their consequences for the surrounding areas.

1. Introduction

When constructing below the groundwater table, there is a risk of groundwater leakage into the structure. To maintain a dry working environment in the facility, the water must be drained away (Cashman and Preene, 2001). Lowering the groundwater pressure level due to drainage can pose a risk of settlement in subsidence-sensitive soils, such as glaciomarine clays, as the pore pressure decreases, and the effective stress consequently increases (e.g. (Langford et al., 2016; Li et al., 2021; Sundell et al., 2019a)). Because the hydraulic conductivity of clay is relatively low, changes in the effective stress can occur slowly compared to more permeable soils where pressure changes may occur instantly. This relatively slow pressure change means that changes in the effective stress and settlements are strongly time-dependent (Terzaghi, 1943). Knowledge on how much and how long groundwater lowering a clay can withstand without causing a critical level of risk for consolidation is crucial when planning and designing measures to counteract these risks.

To enable the risk analysis of pore pressure changes and consolidation due to leakage-induced groundwater lowering, tools are needed to predict the changes in groundwater levels in the hydrogeological system. Numerical groundwater modelling is a tool that enables prediction and understanding of how subsurface constructions can affect flow and pressure levels in surrounding aquifers (Hsiung, 2018; Mok et al., 2024; Sundell et al., 2016). In recent years, uncertainties regarding geological conceptualization have been recognized as the largest source of uncertainty in groundwater modelling (Enemark et al., 2024; Enemark et al., 2019; Refsgaard et al., 2012; Troldborg et al., 2007; Woodward et al., 2016). This means that understanding and representing geology is crucial for obtaining valid and representative results from a groundwater model. Understanding the hydrogeological system and spatial distribution of different hydrogeological units can be achieved through field investigations. However, these are often financially and temporally constrained. Therefore, understanding an area's geological history can effectively be used to complement hard data (Jørgensen et al., 2010).

Unconsolidated deposits in Sweden mainly have a Quaternary origin and were a result of the melting and retreat of the late Weichselian ice sheet 15,000–10,000 years ago (Lundqvist, 1983). Melting is associated with a complex history of coastal displacements, including both transgressions and regressions because of isostatic land uplift and eustatic sea level rise (Lagerlund and Housmark-Nielsen, 1993). Thus, the general stratigraphy in clay-filled valleys below the highest post-glacial shoreline level is thus a result of coastal displacements combined with shifting depositional and climatic conditions due to variations in glacier meltwater quantity and distance to the ice margins (Miller and Robertsson,

* Corresponding author.
E-mail address: Johanna.merisalu@chalmers.se (J. Merisalu).

https://doi.org/10.1016/j.enggeo.2026.108601
Received 27 May 2025; Received in revised form 19 December 2025; Accepted 29 January 2026
Available online 29 January 2026

1988). The stratigraphy of these clay-filled valleys can be divided into two main groups: glacial and post-glacial deposits. Glacial deposits consist of (from bottom to top): glacial till, glaciofluvial material (mainly sand and gravel), and glacio-marine clay. Post-glacial deposits consist of marine clay and/or organic soils, and the top layers of marine abrasion (beach) deposits, organic soils, and/or flood sediments (Bengtsson and Gustafson, 1996). Rapid shifts between transgression and regression during the later stages of the glacial period and early stages of the post-glacial period caused large temporal and spatial variations in the depositional conditions. This resulted in the occasional deposition of sand lenses in the glaciomarine and post-glacial marine clay deposits. The occurrence of sand lenses embedded in clay deposits is expected to be more common in locations with steep bedrock topography. Such areas are present, for example where deep weathering or tectonic processes have resulted in an undulating hilly bedrock relief (e.g., (Lidmar-Bergström, 1995; Migoń and Lidmar-Bergström, 2001)). Such areas are common in glaciated areas with magmatic and metamorphic crystalline bedrock, such as Sweden, Norway, Finland, Canada

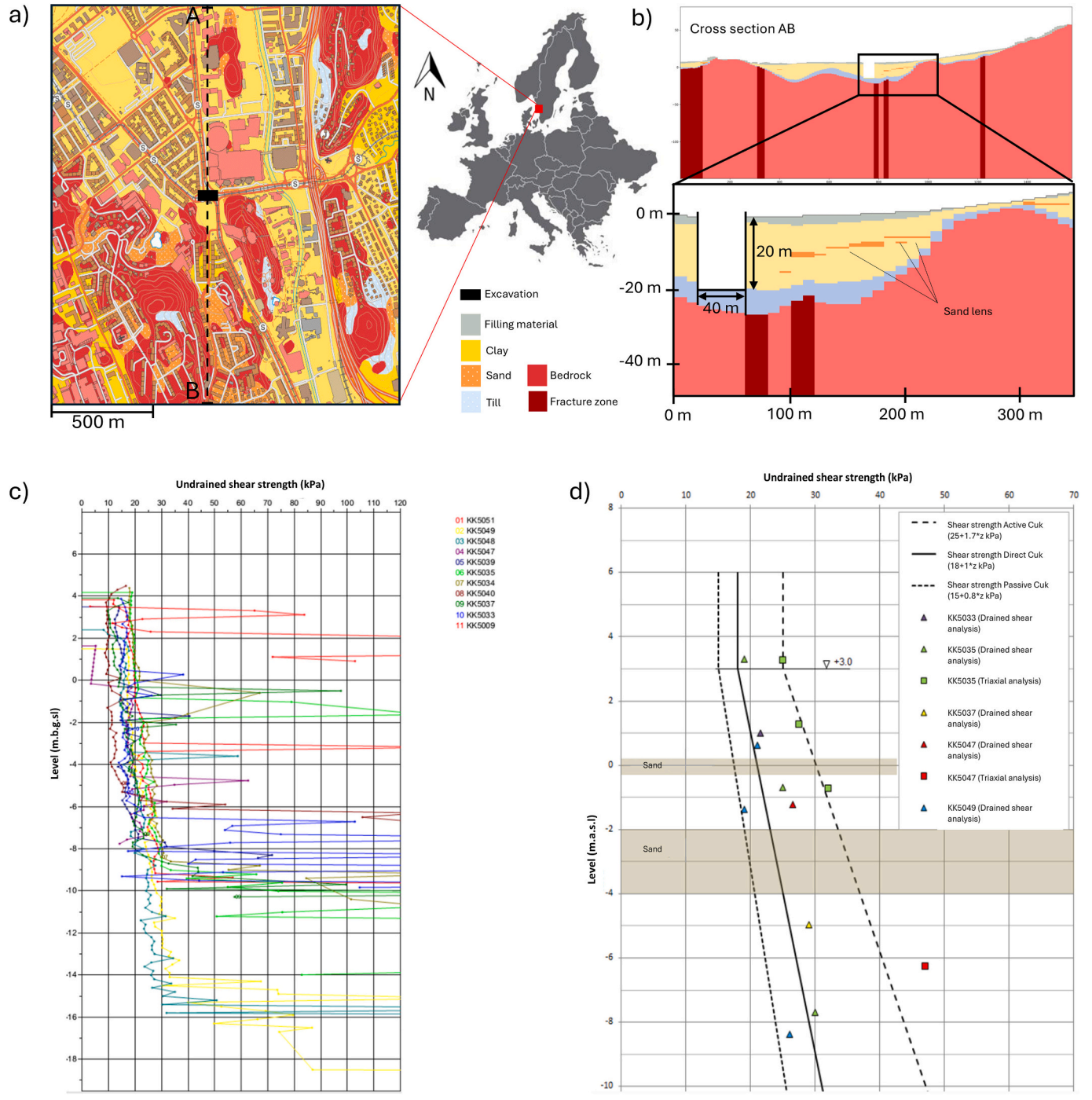

Fig. 1. a) A geological 2D map of the model area in downtown Gothenburg, Sweden, with roads, railways and buildings indicated. The colours in the legend apply to both the planar 2D-map as well as the cross sections. The black square illustrates the site for the excavation and the dashed line the AB cross section that is presented in figure b; b) the AB cross section with the location of the shaft as well as one realization of sand lenses (orange) in clay (yellow); c) the undrained shear strength from cone penetration tests (CPT); and d) the undrained shear strength from soil samples. (For interpretation of the references to colour in this figure legend, the reader is referred to the web version of this article.)

and parts of USA. Due to glacial rebound, substantial areas with such reliefs are now located above sea level.

Permeable units, such as sand lenses embedded in less permeable deposits, can affect the bulk hydraulic conductivity of a stratigraphic sequence (Kessler et al., 2013) and thus increase drainage and settlement rates (Tabarsa, 2017; Urciuoli et al., 2020). The effects on the hydraulic properties mainly depend on how well these units are connected to each other and thus whether these permeable units can form permeable "channels" where groundwater can flow faster than in surrounding low-permeable matrix (Knudby and Carrera, 2005). Not considering these permeable units when predicting groundwater lowering and subsequent pore pressure reduction in subsidence sensitive soils due to leakage may thus result in underestimation of both the magnitude of groundwater lowering and the propagation rate in the system.To the knowledge of the authors, a thorough analysis of the hydraulic importance of sand lenses in glaciomarine clay deposits for predicting pore water pressure change from excavations in urban areas has not previously been performed.

Therefore, the overall aim of this study is to assess the differences in the effects on pore pressure decrease from groundwater leakage into a shaft when accounting, compared to not accounting, for geological model uncertainty. The specific objectives to achieve the overall aim were to *(i)* develop equally probable, geological models based on different geological conceptualizations of the stratigraphy from the same borehole data, where the difference is the clay sequence including or excluding abrasion sand deposits and the location of these deposits, and *(ii)* evaluate the rate and magnitude of the pore pressure change in clay as a function of the geological conceptualization and the location of a synthetic shaft in relation to the permeable sand deposits using numerical groundwater modelling. The final aim is assessing the required complexity of geological models for correct estimation of soil settlements. However, explicit modelling of settlements is not performed in this study.

2. Study site

To study the effect of including and excluding permeable sand lenses in groundwater modelling, an area was chosen where borehole data and deposition history show that sand lenses are present. The model area is located in Gothenburg on the west coast of Sweden (Fig. 1a). The topography of the area varies, with higher bedrock elevations in the east and southwest forming two valleys. In the northern part of the study area the topography is relatively flat. The bedrock is fractured, crystalline metamorphic rock with a heavily weathered and fractured surface. A layer of glacial till and in some locations glaciofluvial coarse-grained sediments overlies the bedrock. Above this, the stratigraphy includes glaciomarine and post-glacial marine clay with thicknesses ranging from a few meters to 70 m in the valleys' deepest sections. Because of the area's complex geological history with coastal displacement and fluctuating sea levels during sedimentation, local and permeable sand lenses can be found at varying depths within and on top of the glaciomarine clay deposit (Stevens and Hellgren, 1990). An example of clay and sand lamina found in a core drilling at the study site is presented in Appendix A. A conceptual interpretation of these types of sand layers is shown in Fig. 1b with orange colour. In Fig. 1c and d, the undrained shear strength in the area is presented from CPT-measurements and from soil samples analysed in lab. Fig. 2, shows an example of a sand layer within clay from the model area. The topmost layer at the ground surface has been heavily altered by weathering and filling materials and is a few meters thick.

3. Method & data

3.1. General approach

The general modelling approach presented in this paper can be summarized into four main steps (Fig. 3). The first step is the development of a conceptual model which includes a description of the hydrogeological setting with focus on geological strata and aquifers, groundwater levels and flows, recharge and boundary conditions (see section 3.2). The conceptual model forms the basis for both the development of geological models and the numerical groundwater models. The second step includes the development of the stratigraphical models which includes one model with a simplified stratigraphy constituting continuous layers and three models constituting a more complex geology where sand lenses are embedded into the clay sequence. The three models including sand constitute three realizations from geological simulations (see section 3.3). These realizations were chosen to illustrate the three conceptual cases of sand layer locations. The third step was the development of the numerical groundwater models where the developed geological models form the basis for the discretization (see section 3.3). The experiment that is carried out investigates differences between geological conceptualization in pore pressure reduction due to groundwater ingress to a synthetic deep excavation (shaft) located in the centre of the model area (see Fig. 1a).

3.2. Conceptual model

The hydrogeology in the area can be summarized into four main aquifers, see Fig. 4. The first aquifer is fractured rock, split into: highly weathered and fractured surficial bedrock with higher hydraulic conductivity, and deeper bedrock with lower hydraulic conductivity. The

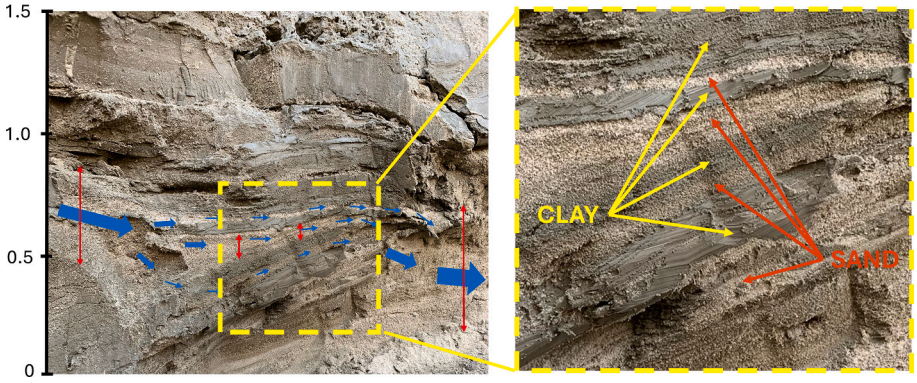

Fig. 2. Images from an excavation at *Korsvägen* in Gothenburg, Sweden. The blue arrows illustrate potential groundwater flow direction, and the red arrows illustrate the variation in height for the sand layers. The unit is meters. The right image is an enlargement of the dashed rectangle highlighting the variation between sand and clay (Original photo by Karl-Martin Iversen, used with permission). (For interpretation of the references to colour in this figure legend, the reader is referred to the web version of this article.)

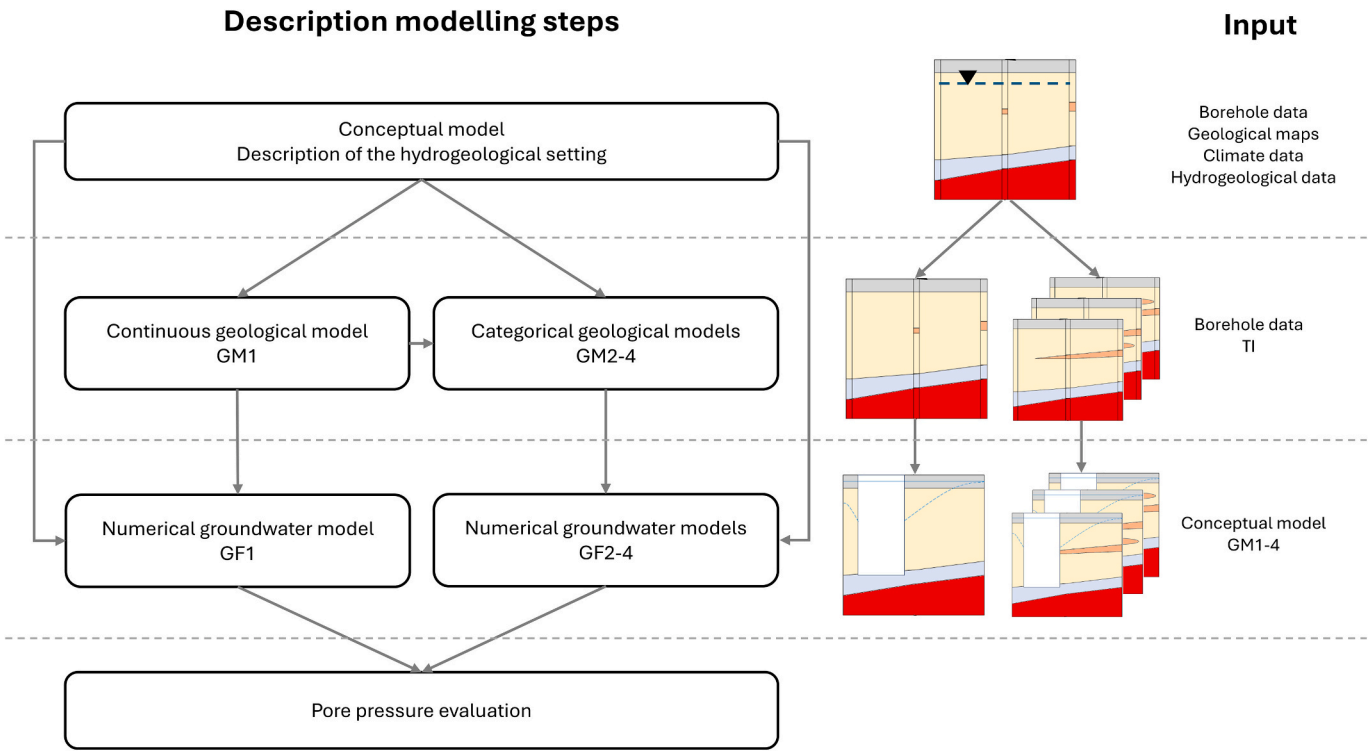

Fig. 3. The general approach to assess the differences in effects on pore pressure decrease from groundwater leakage into a shaft when accounting, compared to not accounting, for local and permeable sand lenses within the clay sequence.

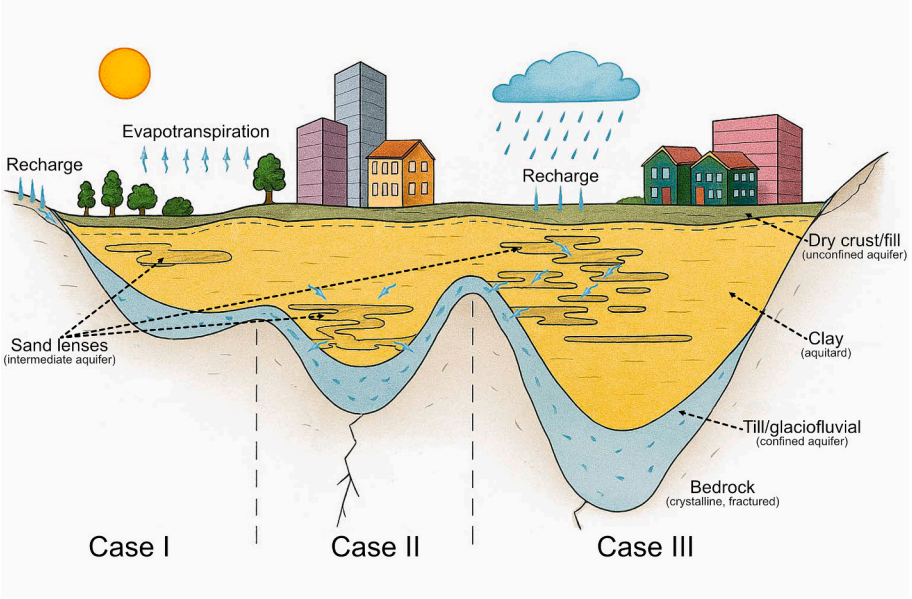

Fig. 4. Illustration of a typical cross section for the investigated hydrogeological setting. The cases I-III represent the geological models (GM2–4) and the Groundwater flow models (GF2–4). The dash line represents the pore pressure in the clay layer.

second aquifer consists of till and glaciofluvial materials, confined by overlying clay. The third aquifer contains confined permeable sand layers and lenses within the clay sequence. The fourth aquifer is the unconfined top layer of sand and fill material. Recharge to the fractured rock aquifer takes place in mainly two ways: 1) precipitation is entering the fractured rock as groundwater recharge in areas with higher altitude and where the rock is bare directly, and 2) groundwater in the confined aquifer is recharging the fractured rock in the lower lying areas (valleys). The confined till and glaciofluvial aquifer is primarily recharged at the valley sides where the aquifer material crops out. There is also an exchange of water between this aquifer and the rock aquifer. The third aquifer constituting sand layers and lenses are covered in more detail below (next paragraph). The fourth aquifer is unconfined and is thus recharged directly from precipitation. The area's high degree of urbanization complicates the flow and recharge of groundwater in the region. Relatively impermeable materials, such as pavements, cover large parts of the area and affect groundwater recharge. Stormwater management and existing underground construction also reduce the possibility of

recharge in the area, whereas leaking drinking water pipes add to groundwater recharge.

The sand lenses and layers that are of focus in this paper have a higher anticipated hydraulic conductivity compared to the surrounding clay. According to Lithén et al. (2016) the median hydraulic conductivity of sand is 4.75^{-5} m/s and clay is 1.9^{-9} m/s. The sand deposits can be classified into three main types:

Case I:

The first case constitutes sand lenses that are isolated by the surrounding clay and may thus be interpreted as intermediate aquifers. These aquifers are only recharged by groundwater flow from the surrounding clay. These types of sand layers are expected to have low impact on the pore pressure changes due to the leakage into the excavation if there is no direct contact with the excavation walls. However, if the excavation is located in contact with these types of sand layers the rate of excess pore water dissipation is expected to increase as the sand layers drain the surrounding clay.

Case II:

The second type refers to sand layers connected to the confined aquifer, functioning as its extension. These lenses are recharged along valley slopes like the main (confined) aquifer. A drop in the aquifer's pressure head within is expected to similarly lower pressure in pressure in these interconnected sand lenses, which can extend reduced pore pressures into nearby clay layers. This effect may increase the risk of settlements and related damages to buildings.

Case III:

the third case involves sand lenses that connect the unconfined and confined aquifers, potentially serving as recharge pathways for the confined aquifer. These connections can help maintain groundwater pressure and prevent pore pressure reductions in overlying clay layers for effective recharge, sand layers must be well connected and located in areas where infiltration occurs. Therefore, Case III scenarios are anticipated in regions with thinner clay layers and permeable land use patterns.

3.3. Geological models

Two geostatistical simulation approaches for creating geological models were used in this study to adequately represent the complexities of the different geological conceptualizations. The first model, which is referred to as geological model 1 (GM1) (see Fig. 3), is a continuous layer model developed with a boundary-based approach, ordinary kriging, detailed in Sundell et al. (2019b). From bottom to top, the stratigraphy consists of crystalline bedrock, frictional material (glacial till/glaciofluvial deposits), glaciomarine clay and filling material, which is a generally accepted hydrogeological conceptualization of the area (Haaf et al., 2024; Lissel, 2016).

The geological models, which include interbedded sand within the clay sequence and are referred to here as geological model 2–4 (GM2–4), see Fig. 3, are based on GM1 but have been further developed using a category-based geostatistical simulation approach. This approach is preferable because it can generate a spatially discontinuous stratigraphy with embedded materials (Xiao et al., 2017). The location and distribution of the embedded sand layers were simulated using Multiple Point Statistics (MPS) (Strebelle, 2002b).

Borehole data was used for the simulation with MPS which required sampling from approximately 1500 boreholes located within the model area. Each borehole was sampled at 0.5-m intervals, focusing on clay deposit data. This resulted in 32,362 data points which were assigned indicator values of 0 or 1, where 0 represents clay and 1 represents sand. Of the total data points, 333 were identified as sand. These data points served as conditioning data for the simulation of sand lens distributions in the geological models containing sand.

Because of the depositional processes, the interbedding of sand layers is expected to be non-stationary across the modelling domain, which can be accommodated by MPS (de Vries et al., 2009). Furthermore, studies have shown that this method is effective in capturing heterogeneities, such as sand lens geometry within deposits (Kessler et al., 2013). Structural realizations will also create more coherent geological units, often making a better representation of actual field conditions (Vilhelmsen et al., 2019). The basic function of MPS is to capture and reproduce the complex spatial patterns and relationships observed in geological datasets (Bastante et al., 2008; Hu and Chugunova, 2008; Liu, 2006; Strebelle, 2002b; Strebelle and Journel, 2001). Unlike traditional geostatistical methods, which generally focus on modelling bivariate statistics (relationships between pairs of points), MPS considers the spatial arrangement of multiple points within a given area. This is done using a training image, a reference that represents the desired spatial patterns and serves to include geological expertise into the simulations. By incorporating prior geological knowledge, e.g., quantitative metrics or conceptual understanding, the training image guides the simulation process, ensuring that the generated models replicate the essential spatial structures and heterogeneities of the system as expected from domain knowledge (Renard, 2007). MPS operates as a stochastic simulation method capable of generating multiple realizations of a geological model.

The training image (TI) used in this study is shown in Fig. 5. The TI was developed using three main inputs:

1) Geological maps of the Gothenburg area:

Abrasion sand deposits are visible at the ground surface close to till covered bedrock outcrops in geological maps. From these, the shape of the deposits can be studied and translated into the TI by interpretation and replication.

2) Knowledge regarding the glacial history of the area:

Abrasion sand deposits were formed during the complex displacement of the shoreline during the last deglaciation. A similar pattern of sand deposits is expected at depth within the clay deposits, since the entire sequence was deposited in the same depositional environment traversing at or below the shoreline.(Agrell, 1979).

3) Borehole data:

The boreholes available for the area also gave information regarding the number of sand lenses that may be present within the clay sequence.

After development, the TI was visually validated using expert judgement to ensure that it incorporated the shapes and distribution of sand lenses that could be expected from the data mentioned above and trial pits (see Fig. 2). Test simulations were carried out to ensure that the simulations generated from the TI together with borehole data was representative for this type of deposit.

The MPS method single normal equation simulator (SNESIM) (Strebelle, 2002a) was employed to generate a total of 50 realizations of the distribution of sand lenses within the clay sequence. Since the purpose of the study was to investigate the difference in including sand lenses in comparison to not include them, three realizations were chosen to constitute the geological models used for the following analysis. These three realizations where manually chosen based on how well they captured the three conceptual cases (Case I-III described in section 3.2) of how sand lenses could contribute to pore pressure decrease induced by leakage into an underground construction.

3.4. Numerical groundwater modelling

Changes in pore pressures within the clay were estimated using the numerical groundwater flow modelling package MODFLOW-NWT (Niswonger et al., 2011). MODFLOW-NWT employs a finite difference approach to solve three-dimensional groundwater flow equations, utilizing a Newton-Raphson formulation to enhance numerical stability and facilitate robust simulation of complex hydrogeological systems. In this study, only the effects of varying geological conceptualizations on pore pressure were considered; ground settlement was not addressed. Consequently, no hydro-mechanical coupling with a constitutive model was implemented, consistent with the initial step in uncoupled methodologies (Li et al., 2020; Pujades et al., 2014).

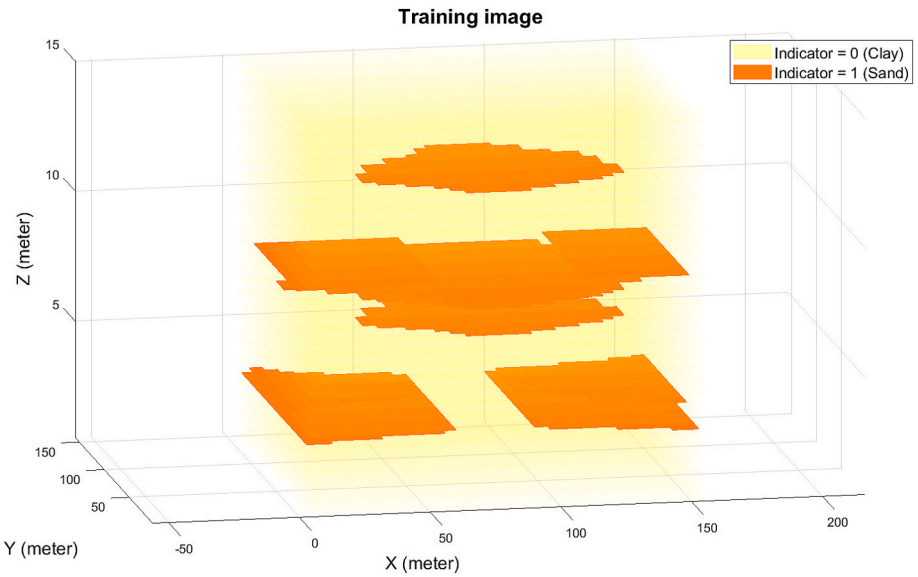

Fig. 5. Illustration of the training image used for the MPS simulations, in two positions. The dimension of the TI is 150x150x15 m distributed over 30x30x30 cells. The orange cells represent sand, and the yellow cells represent clay. The clay is made transparent in the figure to make the sand more visible. The thickness of the sand lenses varies between 0.5 and 2 m. (For interpretation of the references to colour in this figure legend, the reader is referred to the web version of this article.)

The modelling was carried out in two steps: 1) Base models: Integrating the geological models (based on different geological conceptualization) into a numerical groundwater flow model (GWF), including transient calibration on observed pumping tests conducted (without the presence of any shaft/excavation). 2) Forward runs: Simulation of a synthetic scenario introducing a deep excavation into the calibrated models from step 1) for analysing the effects on pore pressure reductions given the different geological. Calibration was also carried out in two steps, first a steady-state calibration on historical records of groundwater head, and second, on the time series of a pumping test prior to excavation activity (Lissel, 2016).

3.4.1. *Setup of base models*

The GWF models were constructed using a voxel-based methodology, in which geological deposits are divided into a three-dimensional structured grid. Each grid cell represents a geological unit that has hydrogeological properties such as hydraulic conductivity and storativity. The model resolution was set to 10 × 10 m horizontally, with a vertical layer thickness of 0.5 m resulting in 158 rows, 173 columns, and 295 layers, allowing a fine-grained description of the geology. This was performed for each geological model resulting in four hydrological models. The model excluding sand within the clay deposit is referred to as GWF1-Clay whereas the models including sand layers are referred to as GWF(2–4)–Sand.

Boundary conditions were assigned to represent the physical limits and hydrological interactions of the study area. No-flow boundaries were applied along the lower boundary and upland ridges, simulating impermeable geological features and groundwater divides. Constant head boundaries were used at the northern and southern edges to mimic natural groundwater inflow and outflow, with head values set based on average groundwater levels. Recharge was incorporated using a specified flux boundary condition at the model top with spatially variable rates based on land use. Anthropogenic influences, such as leakage from drinking water distribution systems, were included as additional recharge sources.

Since the objective of this study was to understand the impact of sand interbedding in the clay deposits on the risks of subsidence due to groundwater lowering. The parameter values were kept constant across the four GWF models, except for the presence of sand. To achieve constant, comparable parameter values while simultaneously ensuring a good fir between observations and simulations, manual, steady-state calibration was carried out. An automated calibration (e.g., PEST) would be in this case counterproductive since it assigns random parameter values to properties in the model according to probability distributions, making direct comparison of model results difficult. Calibration was carried out on groundwater head observations from 150 boreholes, covering both the unconfined and confined aquifers. The head data, which included monthly measurements from 2013 to 2017, were compiled into minimum, maximum, and median values for each borehole. Owing to several ongoing infrastructure constructions at the site, several boreholes showed a clear influence on pumping and infiltration tests with unknown testing periods, flow rates, and locations. Consequently, an ideal match between the observed and simulated head values was not achievable. Instead, the calibration is considered satisfactory when the hydraulic head in all boreholes is within the range defined by the observed minimum and maximum values. In addition, the root mean square error (RMSE) of the median groundwater level must meet the criteria based on the maximum difference in potentials within the model area as well as an ambition level for detailed modelling according to the Danish guidelines for groundwater modelling (Refsgaard et al., 2010). For this model area and use, the RMSE should not exceed 0.9 m.

After achieving this calibration threshold, a transient simulation was carried out based on the steady-state simulation as the initial state. The transient models were calibrated on a pumping test carried out at the excavation shaft location (see Fig. 1a). The Pumping test was conducted for two weeks and the calibration included four observation points with different directions and distances to the pumping well. This calibration was deemed satisfactory when the simulated drawdown at all observations points was in line with the observed drawdown based on visual comparison.

3.4.2. *Forward run and pore pressure evaluation*

For the forward runs, a shaft was introduced to the model constituting a 20 m deep and 40-m-wide open excavation, implemented using the drain package (DRN) and Horizontal Flow Barriers package (HFB). The DRN package simulates dewatering at the bottom of the shaft with a head-dependent flux (Cauchy) boundary. The HFB package is used to control the permeability of the excavation walls and is set to a conductance of 10^{-10} ms^{-1}, allowing water to enter the shaft. The

effects on pore pressure in the clay layer as a result of the simulated leakage of water into the shaft and the removal of this water were evaluated for all models (GWF1, GWD2–4) through transient groundwater modelling with five time steps. The time steps were set to 1 day, 1 week, 1 month, 1 year, and 30 years to allow for an evaluation of pore pressure changes both in both at short and long term. The change in pore pressure change was calculated using Eq. 1:

$$\Delta u = (hi - h_t)g\rho \quad (1)$$

where.

Δu – pore water pressure change (Pa),
h_i – initial hydraulic head (m),
h_t – hydraulic head at different time steps (m),
g – gravitational acceleration (m/s^2), and.
ρ – density of water (kg/m^3).

4. Result and discussion

4.1. Groundwater modelling

Fig. 6a and b show the results of the steady-state calibration for GWF2-Sand and GWF1-Clay. This shows that the simulated groundwater levels for both the unconfined and confined aquifers generally corresponded to the observed levels. All models had an RMSE within the range of 0.68–0.70 m, which is lower than the target of 0.9 m, and therefore, the manual calibration of the stationary conditions was considered satisfactory. The resulting head distribution from the steady-state calibration, used as the initial conditions, is shown in Fig. 6c. However, small differences between the models are observed in Fig. 6a and b. For example, at the observed level of 12 m, the model including sand shows a simulated level approximately 1 m lower than GWF1-Clay. This could be because the sand layers in GWF2-Sand are relatively close to the unconfined aquifer, potentially diverting water from the unconfined aquifer to the confined aquifer.

Fig. 6c and d show the results of manual transient calibration. In Fig. 6d, between days 8 and 11, recurring stops at the pumping station

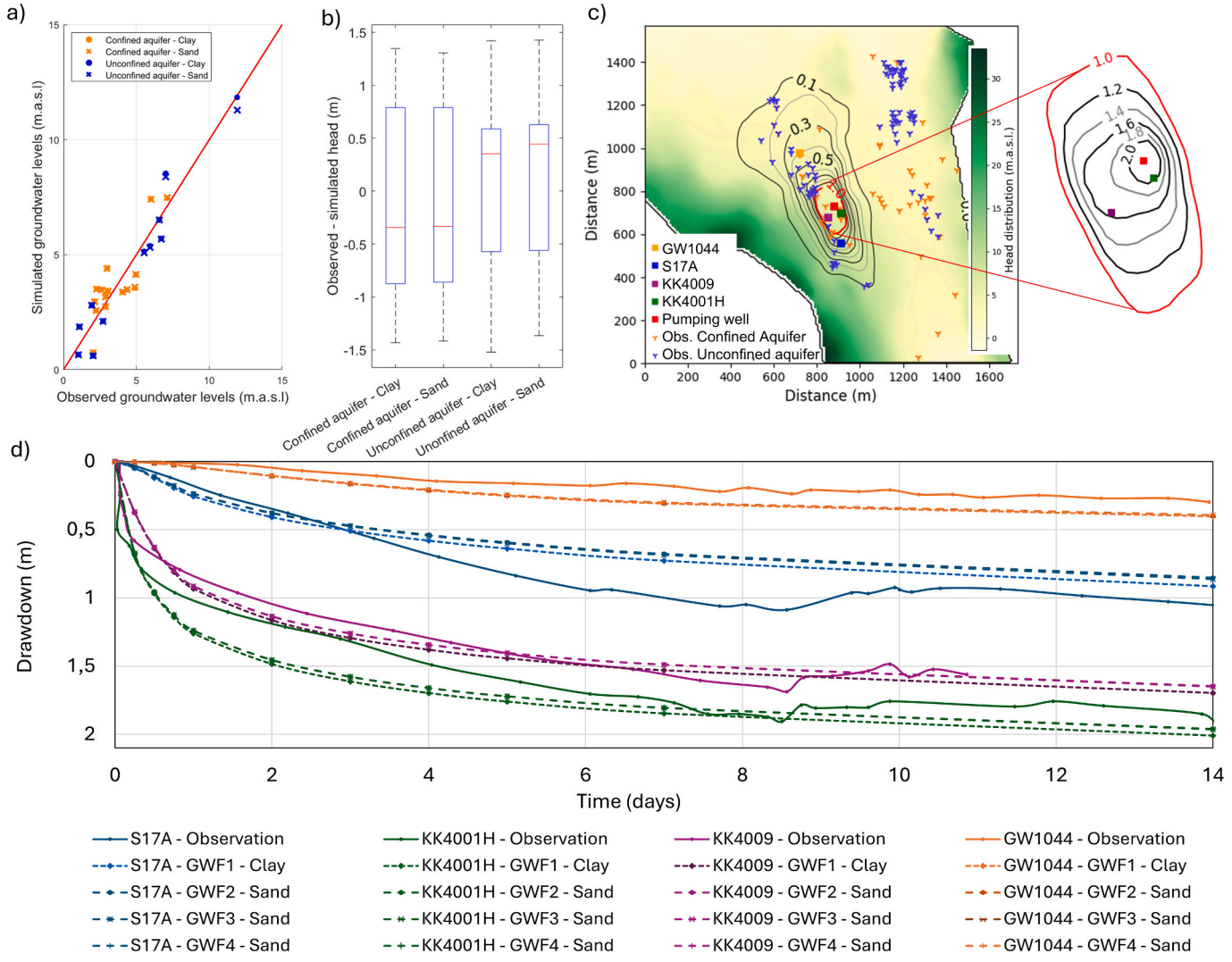

Fig. 6. a) Observed groundwater levels vs simulated groundwater levels for GWF1-Clay and GWF2-Sand for the steady state calibration. b) The difference in head for observed and simulated groundwater levels for the steady state calibration. Both figure a and b show the result for 26 out of 151 wells. All wells were used for the calibration but for the plots, only one well within a radius of 15 m was chosen for visualization. c) The locations for the observation wells and pumping well, the simulated head distribution from the steady state calibration with a colour scale, and the simulated drawdown for the transient calibration for GWF2-Sand with contour lines. d) The observed (solid line) and simulated drawdown (dashed lines) for all groundwater models (GWF1–4) in observation wells S17A, KK400iH, KK4009, and GW1044.

caused similar drawdown fluctuations in all the observation wells. At well GW1044 (Fig. 6d), the observed fluctuations also suggest an unaccounted recharge, possibly from an infiltration facility or leaking water pipes, which could explain why the simulated drawdown exceeded the observed levels. In contrast, the simulated drawdown is less than that observed in well S17A after three days, suggesting a lower recharge than the simulated models. This may be due to local stormwater management not accounted for. However, the calibration aims for a realistic response rather than site-specific accuracy, and overall, the models align well with the observations, indicating a reliable groundwater flow representation.

The calibrated hydrogeological parameters and recharge values for the stratigraphic units within the models are presented in Fig. 7. As illustrated by the figure, most calibrated values fall within or close to the ranges established by field investigations and literature. These ranges generally represent the referenced values; however, in in some cases they also pertain to adjacent units. For instance, the values determined for weathered bedrock may also be indicative of the overlying till and glaciofluvial materials as hydraulic testing makes it difficult to distinguish between these layers when assessing hydrogeological properties.

The calibrated hydraulic conductivity value for fracture zones falls outside the specified range. However, this range reflects the variability in hydraulic conductivity across the Gothenburg area. According to Lissel (2016) and Lithén et al. (2016), the fracture zones at Korsvägen are frequently filled with clay minerals, which results in a lower hydraulic conductivity compared to the general conditions in the Gothenburg area.

The calibrated values for specific storage for clay, sand, and glacial till and glaciofluvial deposits are within the range of the literature values from the Gothenburg area albeit at the lower end. This can be explained by the higher consolidation in our area compared to other areas with thinner soils. Similarly, the calibrated values for specific yield are in general lower compared to the literature values which can be explained by the frequent content of finer fractions (clay and silt lamina) in the coarser sediments. It is important to note that, due to the construction of the groundwater model in which the upper part of the bedrock is represented as a separate layer (weathered bedrock), recharge occurs only in the weathered bedrock layer and not in the bedrock layer or fracture zones.

4.2. *Effect of sand lenses on pore-water reduction*

The modelling showed four different situations in which sand lenses impacted the magnitude and rate of pore pressure reduction owing to a lowered groundwater head in the confined aquifer. Two cases were related to isolated sand lenes, indicating that there was no connection to other permeable deposits (Fig. 8a and b). The pore pressure reduction in clay in Fig. 8a shows little differences between the models including and excluding the sand layers. However, in b, where the isolated sand layer is connected to the retaining walls, the reduction in pore pressure for GWF3–Sand is much higher compared to GWF1-Clay. The sand layer, located at a depth of nine meters, acts as a drainage path for water in the clay into the shaft, resulting in a significantly larger and faster pore pressure reduction in the clay sequence. This result indicates that the location of the sand lens in relation to the location of the shaft plays a major role in the evolution of pore pressure decrease. Thus, sand lenses isolated in the clay are not of high importance unless they are cut by the excavation wall.

The remaining two cases were related to sand layers connected to the confined aquifer (see Fig. 9a and b). The consistent reduction at both the sand layer levels and bottom of the graphs indicates that the sand layers act as an extension of the confined aquifer, substantially affecting the pore pressure reduction in the surrounding clay. As shown in Fig. 9a, the sand layer that is connected to both the confined aquifer and retaining wall has a lower decrease in pore pressure in the clay sequence compared to GWF1-Clay. This positive effect on pore pressure due to the sand layers is a consequence of the hydraulic head in the confined aquifer being higher than the unconfined level of the sand layer allowing groundwater to flow from the confined aquifer to the sand layers, i.e., the confined aquifer recharge the sand layer. In other words, the saturated sand layer with a high hydraulic head maintains the pore pressure in the overlain clay while in the model without this sand layer. However, if the hydraulic head were to be lower than the level of the sand lens, the recharge to the sand layer would be limited. Therefore, it could instead work as a drain in the surrounding clay, increasing the rate of pore pressure reduction. Fig. 9b shows that the sand layer stretches out from

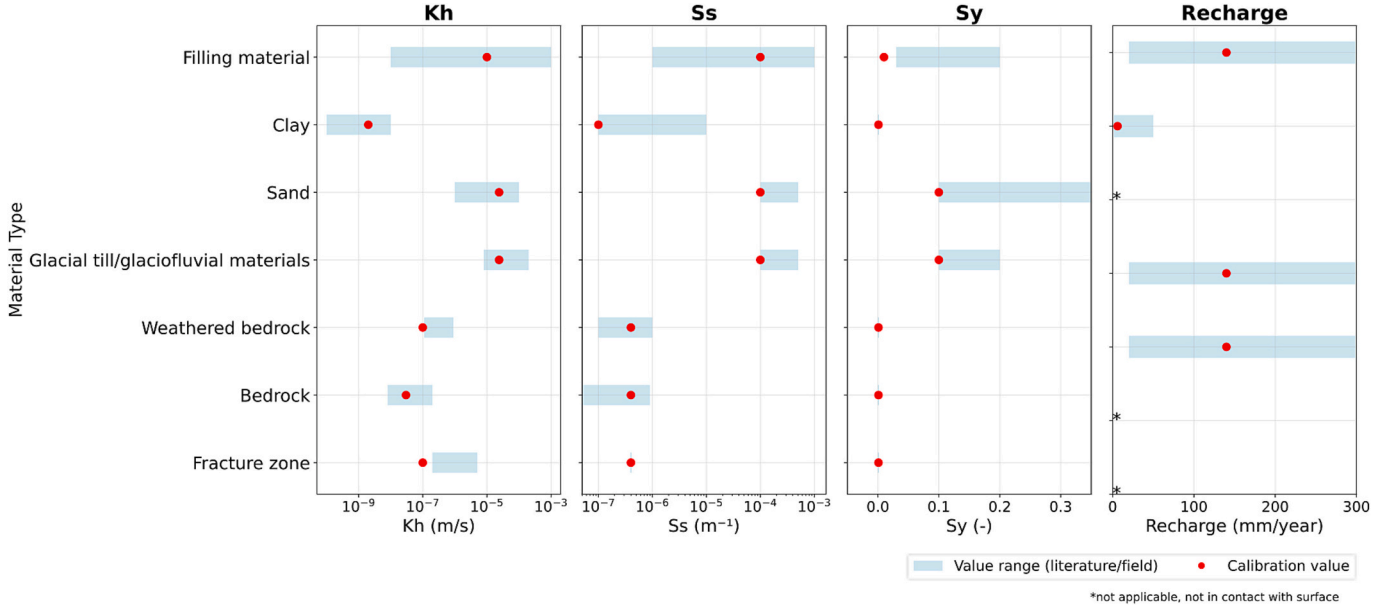

Fig. 7. The resulting parameter values from the calibration for horizontal hydraulic conductivity (*Kh*), specific storage (*Ss*), specific yield (*Sy*), and recharge are compared to values obtained from field investigations and literature. All values are based on field investigations reported by the Swedish Transport Administration (Haaf et al., 2025; Lissel, 2016; Lithén et al., 2016; Sundkvist, 2016) or Fetter Jr (2001). Vertical hydraulic conductivity was assumed to be equal to *Kh* except for filling material and Clay (Kh/2).

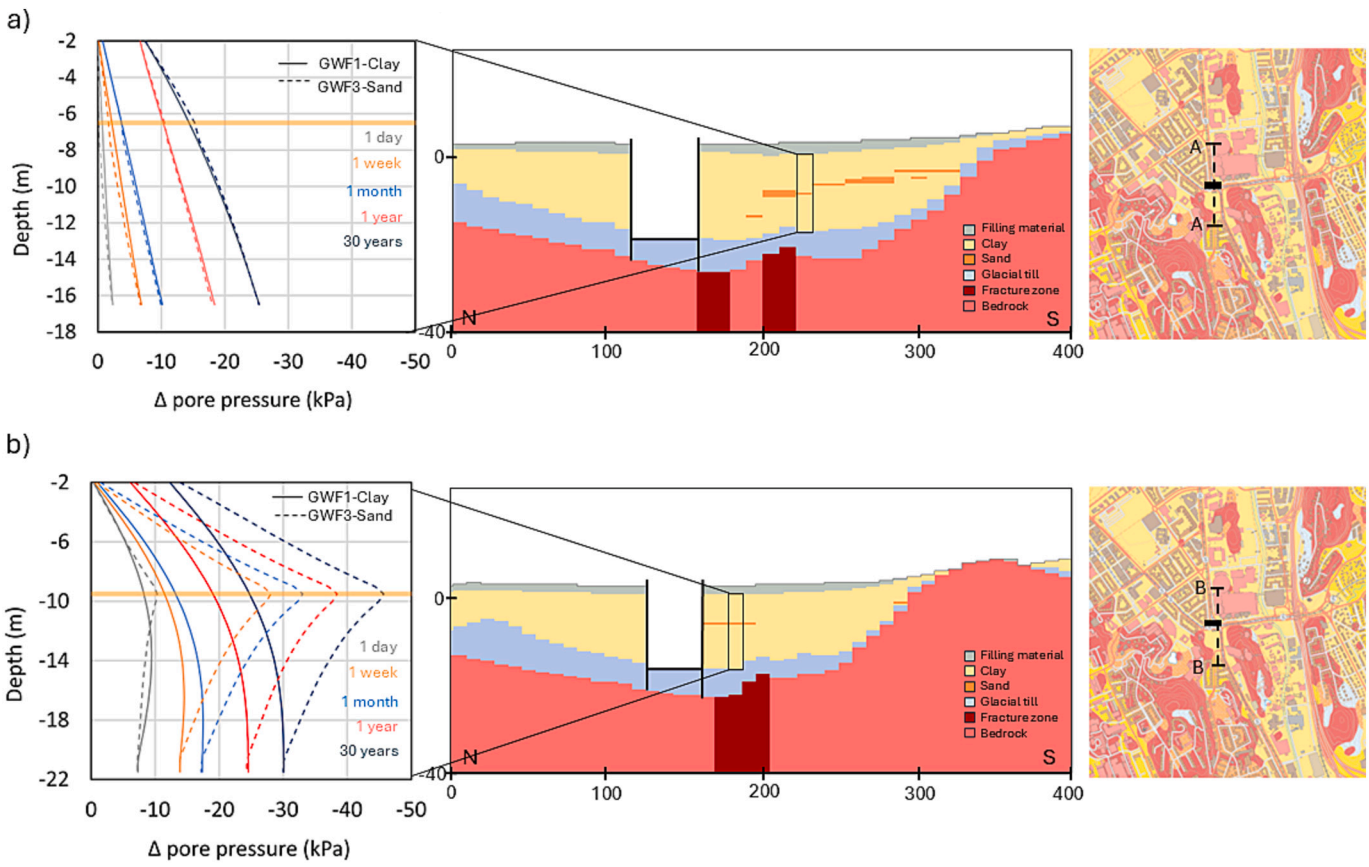

Fig. 8. The left figure shows the pore pressure reduction profiles for GWF1-Clay and GWF3-Sand at time steps of 1 day, 1 week, 1 month, 1 year, and 30 years. The yellow horizontal line indicates the location of the sand layer. The dashed line represents GWF3 with sand lenses, while the solid line represents GWF1-Clay. The middle figure presents a cross-section of the stratigraphy in the surrounding area corresponding to the reduction profile. The right figure indicates the cross-section's location within the model area, along with the position of the excavation shaft. (For interpretation of the references to colour in this figure legend, the reader is referred to the web version of this article.)

the confined aquifer, extending to a higher elevation. Because the pressure head reduction in the sand layer is the same as in the confined aquifer, the higher level of sand contributes to the pore pressure reduction propagating upwards faster in the clay sequence. This result indicate that sand lenses connected to the confined aquifer works as an extension of the confined aquifer and should not be seen as an isolated aquifer. This also indicates that the pressure head in the confined aquifer plays a major role in how the sand layers impact the pore pressure in the overlain clay.

The results presented in this section are all a product of the expert-based conceptualization of the distribution and shapes of sand lenses in clay in this hydrogeological setting. However, there might be other cases that were excluded with this method. There may also be subdivision within each case (isolated and connected to the confined aquifer) regarding shape, size, distribution, location and connectivity that has not been included in this analysis. Other methods, e.g., quantitative connectivity metrics (see e.g., (Renard and Allard, 2013; Rizzo and de Barros, 2019) may have the potential to better characterize the cases.

4.3. Implications

Pore pressure changes caused by groundwater leakage during underground construction can lead to significant ground settlements, affecting both structural integrity and project costs. To mitigate such risks, a thorough risk assessment is essential for effective planning and cost management (Merisalu et al., 2023). The results from this study shows that there are important differences between the inclusion and exclusion of local and thin sand layers within the clay sequence in groundwater modelling. This conclusion is also supported by other studies. As a first example, Kessler et al. (2013) showed how sand lenses in tills form flow paths and thus increased the bulk hydraulic conductivity of the soil. Urciuoli et al. (2020) showed how thin permeable layers significantly alter drainage and pore pressure dissipation in layered soil. Tabarsa (2017) showed that sand lenses in clay significantly accelerated pore pressure dissipation and altered settlement patterns and that sand lenses therefore must be accounted for in geotechnical design and modelling. In a broader context, permeable layers and clay lenses can also increase the risk of piping (Chen et al., 2020; Li et al., 2022; Zhu et al., 2023). Permeability of clays are also a key parameter in the risk of groundwater buoyancy (Liu et al., 2024; Sun et al., 2023).

As indicated in this study, the potential consequences of sand lenses depend on their location relative to the excavation and other permeable materials, as well as to pressure levels in the sand and in connected aquifers. The calibration shows only minor differences between the assumptions of excluding and including sand layers in groundwater modelling. This was expected because the calibration was based on observed water levels in the unconfined and confined aquifers, where the largest pore pressure differences occurred within the clay sequence. Although the results showed minor differences during calibration, Fig. 6a highlights that sand layers increase the recharge to the confined aquifer. Excluding these sand layers could underestimate the recharge to the confined aquifer and subsequently overestimate the pore pressure reduction in the overlaying soil, potentially exaggerating subsidence risks and leading to unnecessary mitigation costs.

Sand layers with no connection to other permeable layers generally have a limited impact on pore pressure reduction (Fig. 8a). However, the

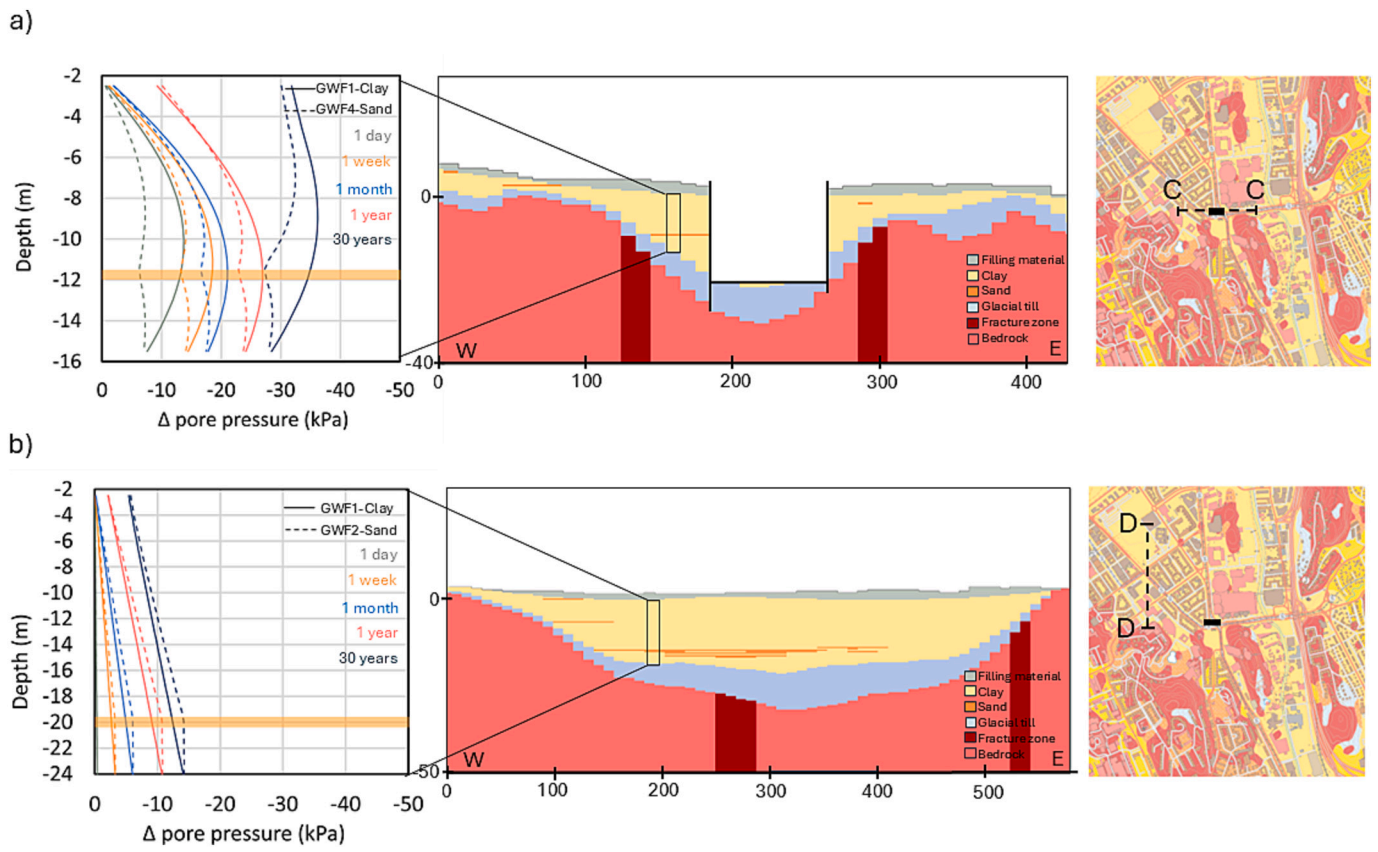

Fig. 9. The left figure shows the pore pressure reduction profiles for GWF1-Clay and for GWF2-Sand and GWF4- Sand at time steps of 1 day, 1 week, 1 month, 1 year, and 30 years. The yellow horizontal line indicates the location of the sand layer. The dashed line represents the model with sand layers, while the solid line represents GWF1-Clay. The middle figure presents a cross-section of the stratigraphy in the surrounding area corresponding to the reduction profile. The right figure indicates the cross-section's location within the model area, along with the position of the excavation shaft. (For interpretation of the references to colour in this figure legend, the reader is referred to the web version of this article.)

situation changes considerably if these layers are connected to the open excavation, because they can act as efficient drainage paths for the surrounding clay (Fig. 8b). This lead to rapid pore pressure changes and may lead to accelerated consolidation, which can cause ground deformations and affect the ground stability in the surrounding area. Sandene et al. (2024) identified pore pressure reduction owing to leakage during the installation of tie-back anchors and bored piles as one of the most common causes of unexpectedly large settlements in deep excavations. This indicates that leakage paths can occur during these installations. If permeable sand layers can also be drilled through and drained, the risk of significant and rapid pore pressure reduction increases during these types of installations. Excluding these sand layers thus risks underestimating the rate of pore pressure changes in the clay during the construction phase, even at an early stage.

Sand layers with a connection to the confined aquifer can both increase and decrease the pore pressure reduction compared with a homogeneous clay profile (see Fig. 9a and b). If a sand layer is hydraulically connected to both the excavation and confined aquifer, it can function as a flow path for groundwater, provided that the pressure level is sufficiently high. In this scenario, the sand layer acts as a buffer for the pore pressure in the surrounding clay, thus counteracting pore pressure reduction. However, if there is no hydraulic connection with the excavation, a sand layer that is connected to the confined aquifer may instead act as a drainage path, thereby increasing pore pressure reduction in the surrounding clay. In areas with deep clay layers, sand layers extending from the confined aquifer can significantly shorten drainage paths. This leads to faster and more extensive changes in pore pressure, which can affect the settlement process (Haaf et al., 2024). Because of the formation process of these sand layers, it is likely that they extend from glacial and/or glaciofluvial sediments, meaning that they are found both in areas with thinner clay sequences and where the thickness of the clay increases. Wikby et al. (2024) showed that these areas, where the thickness of the clay sequence increases, tend to be particularly sensitive to settlement, because of the interplay between clay thickness and its consolidation history. Therefore, the level of the sand layer in relation to the unconfined and confined aquifers is critical, as it determines the length of the drainage paths within the clay. This highlights the risk of significantly underestimating settlement risks when permeable sand layers are excluded from predictions of the impact of underground constructions in hydrogeological environments similar to the one studied here.

These results highlight the risks of excluding permeable sand layers in impact predictions for underground constructions in similar hydrogeological environments. Even with limited pressure changes, the presence of sand layers can have a significant impact depending on their location and connection to other permeable materials. The inclusion of these types of heterogeneities within the clay deposit is therefore essential in groundwater modelling and risk assessments to achieve more accurate predictions of pore-pressure reductions in soft soils, settlement risks, and their consequences for surrounding areas.

4.4. *Uncertainties and further research*

The conceptualization of geology is often recognized as one of the largest sources of uncertainty in groundwater modelling (Bredehoeft, 2005; Refsgaard et al., 2012). Uncertainties caused by unknown local-scale stratigraphic heterogeneity is a part of the overall conceptual geological uncertainty and can play a significant role and should

somehow be considered when assessing predictive uncertainties of groundwater heads (Troldborg et al., 2021). This is in line with this study as the results show that the inclusion of thin sand layers can have a significant impact on simulated pore pressure reduction. However, this does not necessarily mean that these layers always should be included in groundwater modelling. The decision depends on the level of accuracy required to identify risks and make well-informed decisions regarding construction and potential mitigation measures. In some cases, a highly simplified model may be sufficient to estimate the order of magnitude of pore pressure reductions in areas where the consequences of misjudgements are not particularly severe. However, this is rarely the case in urban environments, where even small reductions in the pore pressure can have significant consequences (Liu et al., 2022; Sundell et al., 2019b; Wikby et al., 2024).

To incorporate these types of heterogeneities into models and risk analyses, a systematic and thorough data-collection process is required. This places demands on both sampling methodology and the interpretation of the results from these investigations (Troldborg et al., 2021). Because different clients have varying goals and requirements depending on the purpose and scope of the project, it is crucial to define what information is necessary to ensure an accurate representation of subsurface conditions at the planning stage of the geotechnical investigations. Therefore, it is essential to highlight the importance of identifying and documenting heterogeneities, such as the distribution and characteristics of sand layers, during sampling. This means that sampling should be conducted using methods that capture variations in soil stratigraphy and that personnel carrying out the investigations are aware of the significance of these structures. However, even with carefully executed sampling, accurately representing the presence and continuity of sand layers remains challenging. Therefore, further probabilistic modelling is recommended to better understand uncertainties related to the location and connectivity of sand lenses, as well as to reduce uncertainties associated with the quality and quantity of available borehole data (Liu and Wang, 2022; Troldborg et al., 2021). Such methods enable a more reliable risk analysis of subsidence caused by groundwater drawdown. By integrating these insights into groundwater modelling, settlement risks can be assessed more accurately, providing a more comprehensive evaluation of the potential impacts on the surrounding areas.

In this study, data indicating the presence of sand layers were available, yet this information was not included in the groundwater modelling for the ongoing infrastructure project in the area (e.g. (Lissel, 2016)). The results of this study demonstrated that the inclusion of these sand layers has a significant impact, highlighting that valuable information is being overlooked. Information on these types of heterogeneities is crucial, both during the planning phase and throughout the construction of underground projects. In this study, data on these sand layers were already available. However, to better understand whether this type of information provides added value and whether additional data collection is necessary, a more structured Value of Information Analysis (VOIA)(Freeze et al., 1992) is recommended, following, for example, the procedure presented by Sundell et al. (2019c). By applying VOIA, it is possible to determine whether further data collection or a more comprehensive analysis of existing hydrogeological information is justified in relation to the potential consequences of the uncertainties. This type of analysis is particularly relevant for infrastructure projects in urban environments, where small variations in geological parameters can have significant economic and safety implications. Overlooking information on heterogeneities, such as the presence of sand layers, can lead to suboptimal decisions and increased costs throughout the project, which VOIA can help identify and mitigate.

The reasons why heterogeneities are often overlooked in modelling are many and include economic factors, technical limitations such as the lack of available software, and misunderstandings regarding the complexity and time required to incorporate them into models. Nearly 20 years ago, Renard (2007) highlighted the potential of geostatistics in hydrogeology, emphasizing MPS as a promising simulation method. Renard pointed out that geological point data alone are often insufficient for creating a realistic model. However, using MPS, point data can be combined with geological expertise to generate realistic models that incorporate complex geological conceptualizations. He also emphasized that despite its great potential, there remains a significant gap between academic research and conventional applications. Although advancements in geostatistics within hydrogeology have been substantial since then, the divide between academia and practical usage remains large even today. However, this study proposes a relatively straightforward method to integrate such data, improving the reliability of models and their ability to predict groundwater dynamics. By incorporating heterogeneities, this approach can enhance risk assessments, offering better insight into how complex geological conditions influence groundwater systems without making modelling prohibitively resource-intensive.

5. Conclusions

This study evaluated the effect of neglecting thin sand layers within clay deposits on the magnitude and rate of simulated pore pressure reduction due to groundwater drawdown following leakage into a deep excavation. Different situations were identified in which interbedding sand layers should be considered in groundwater modelling and risk analysis for groundwater drawdown-induced settlements. Practitioners should consider following factors when assessing the relevance of sand interbedding in soft soils from a subsidence-risk perspective:

- **Sand Lenses Near Excavation:** Sand lenses near excavation can cause significant variations in pore pressure changes compared to when these layers are not included. Isolated sand lenses near the excavation wall can significantly increase both the rate and magnitude of pore pressure reduction in the clay sequence, as they act as drainage for the surrounding clay.
- **Complex Effects of Hydraulically Connected Sand Lenses:** Sand lenses that are hydraulically connected to other permeable materials exhibit more complex effects. Such lenses can act as drainage paths that enhance pore pressure reduction and as flow paths that maintain pore pressure in the surrounding clay.
- **Impact of Sand Lenses Connected to the confined Aquifer:** Sand lenses connected to the confined aquifer were found to have a particularly large impact on both the rate and magnitude of pore pressure reduction in the overlying clay, even in the absence of direct connection to the excavation. These layers act as extensions of the confined aquifer, indicating that the level of the sand lens can significantly increase the propagation of pore pressure reduction in the overlying clay sequence.

This indicates that careful characterization of sand interbedding in clay and accurate geological representation in simulation models for pore pressure changes can influence outcomes. If these geological uncertainties are not considered, settlement risks may be misestimated, which could result in inaccurate cost projections. Finally, the presented methodology, combining geological conceptualization, geological knowledge-based modelling with MPS and groundwater flow modelling can be used as a blueprint for engineers investigating the impact of interbedding structures with conductivity contrasts on settlement risks.

CRediT authorship contribution statement

Sofie Axéen: Writing – review & editing, Writing – original draft, Visualization, Validation, Software, Methodology, Formal analysis, Conceptualization. **Johanna Merisalu:** Writing – review & editing, Writing – original draft, Visualization, Validation, Supervision, Software, Methodology, Funding acquisition, Formal analysis, Conceptualization. **Ezra Haaf:** Writing – review & editing, Validation, Supervision, Funding acquisition, Conceptualization. **Lars Rosén:** Writing – review &

editing, Validation, Supervision, Project administration, Funding acquisition, Conceptualization.

Funding

This work was funded by the Swedish Rock Engineering Research Foundation (contract BeFo 414) and the Swedish Research Council for Sustainable Development Formas (contract no 2022–01074).

Declaration of competing interest

The authors declare that they have no known competing financial interests or personal relationships that could have appeared to influence the work reported in this paper.

Appendix

Grain size distributions for 43 samples taken from one core (the Liseberg core) at Korsvägen is presented in Fig. A1-A3. The grain size distributions were originally published by Claesson (2022). Three AMS ^{14}C datings of mollusc shells indicate that the core time frame was 6000–10,000 14C years BP. The grain size analysis was only performed for finer sediments, i.e. the analysis did not include sediment fractions >63 μm. The sand-sized fraction estimated in this study was, in addition to sand, also including organic and calcareous materials, such as faecal pellets and foraminiferal shells

For the lowest part of the core (subsamples taken at 22.59 m, 24.24 m, 30.12 m and 32.32 m depth from land surface) the clay content is approximately 62–68% and the sand fraction content is between 1 and 21%. In samples taken at 20.85 m, 20.87 m, 21.65 m and 21.67 m depth, the clay content fluctuates between 23 and 63% and the sand fraction varies between 2 and 19%. In the section between 12.0 and 20.5 m depth the clay content is generally higher, and the sand fraction is reduced to 2–7%. Between 14 m and 18 m depth, the grain size changes to more clayey fractions with a lowest measure of clay content of 77% and a highest measure of 91%. The sand fraction decreases to less than 1% for all subsamples between 14 m and 18 m depth. In the 2–14 m upper core section, the clay content decreases to approximately constant values of 64–76%. The sand fraction is less than 4%.

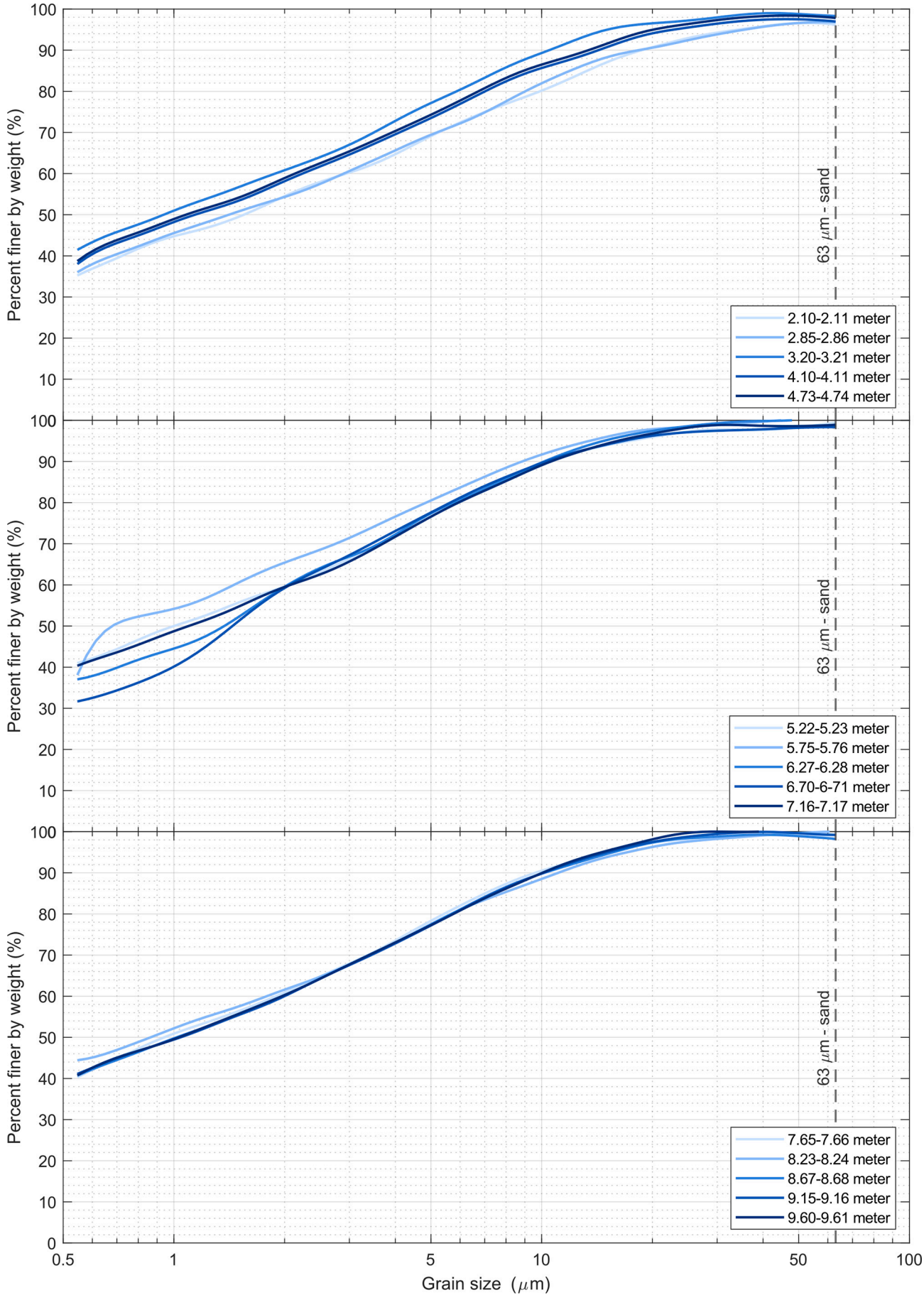
Percent finer by weight (%)
63 μm - sand
2.10-2.11 meter
2.85-2.86 meter
3.20-3.21 meter
4.10-4.11 meter
4.73-4.74 meter
5.22-5.23 meter
5.75-5.76 meter
6.27-6.28 meter
6.70-6-71 meter
7.16-7.17 meter
7.65-7.66 meter
8.23-8.24 meter
8.67-8.68 meter
9.15-9.16 meter
9.60-9.61 meter
0.5
1
5
10
50
100
Grain size (μm)

Fig. A1. Grain size distribution for 15 subsamples from a total of 43 subsamples from the Liseberg core.

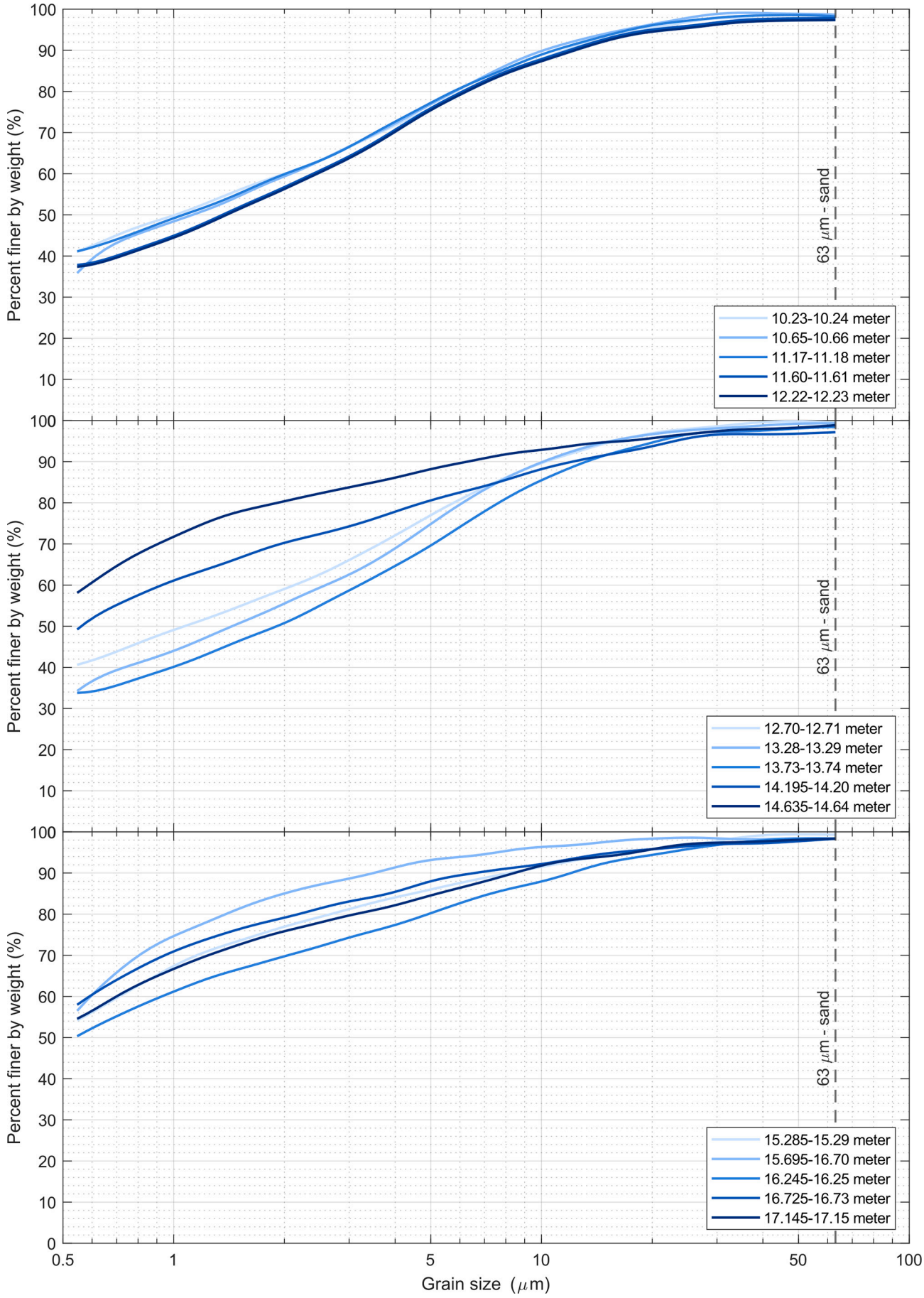
Percent finer by weight (%)
63 μm - sand
10.23-10.24 meter
10.65-10.66 meter
11.17-11.18 meter
11.60-11.61 meter
12.22-12.23 meter
12.70-12.71 meter
13.28-13.29 meter
13.73-13.74 meter
14.195-14.20 meter
14.635-14.64 meter
15.285-15.29 meter
15.695-16.70 meter
16.245-16.25 meter
16.725-16.73 meter
17.145-17.15 meter
0.5
1
5
10
50
100
Grain size (μm)

Fig. A2. Grain size distribution for 15 subsamples from a total of 43 subsamples from the Liseberg core.

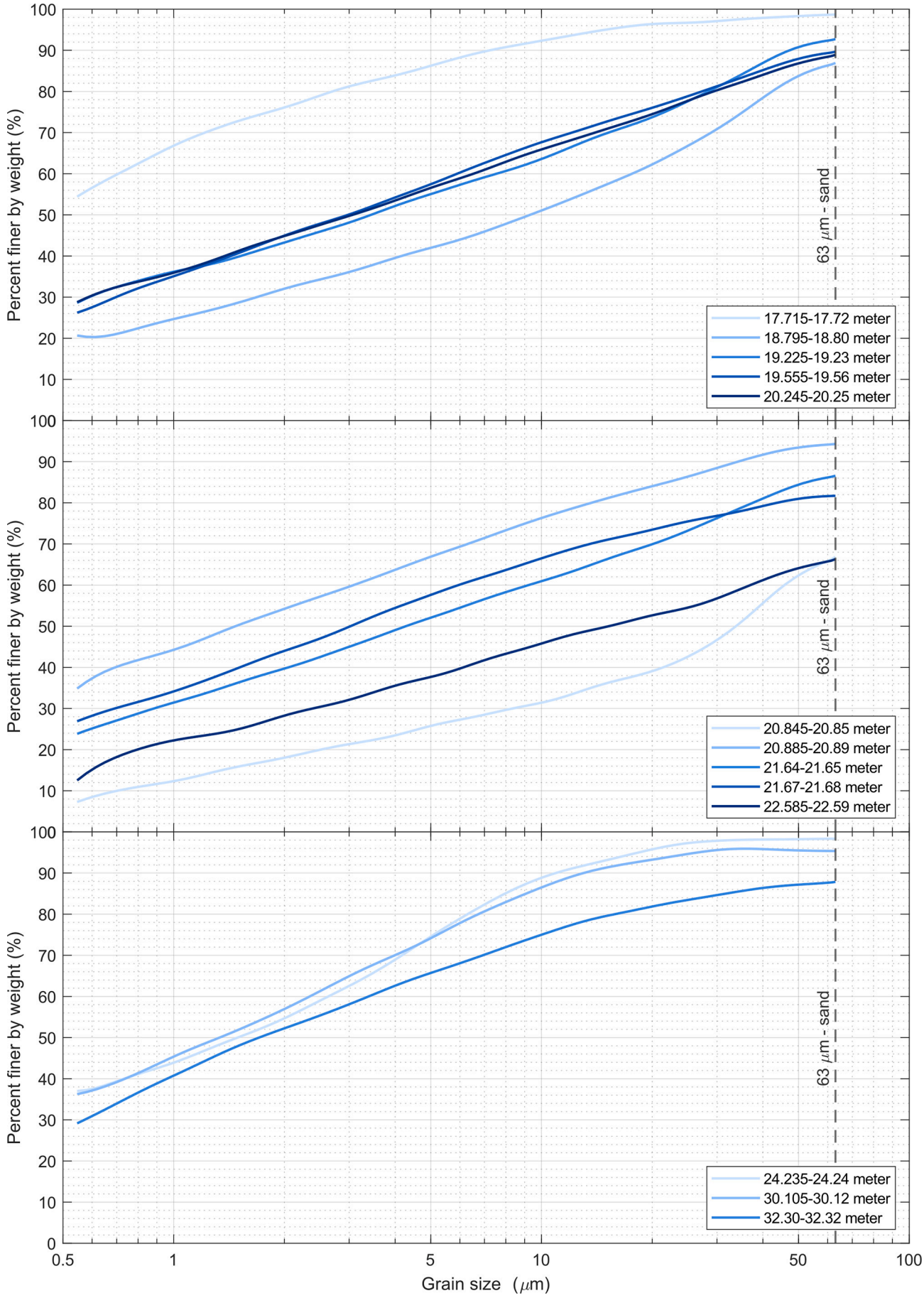
Percent finer by weight (%)
63 μm - sand
17.715-17.72 meter
18.795-18.80 meter
19.225-19.23 meter
19.555-19.56 meter
20.245-20.25 meter
20.845-20.85 meter
20.885-20.89 meter
21.64-21.65 meter
21.67-21.68 meter
22.585-22.59 meter
24.235-24.24 meter
30.105-30.12 meter
32.30-32.32 meter
0.5
1
5
10
50
100
Grain size (μm)

Fig. A3. Grain size distribution for 13 subsamples from a total of 43 subsamples from the Liseberg core.

Data availability

Data will be made available on request.

References

Agrell, H., 1979. The Quaternary of Sweden, vol. 770. Sveriges Geologiska Undersökning. https://books.google.se/books?id=Az6sPAAACAAJ.

Bastante, F., Ordóñez, C., Taboada, J., Matías, J., 2008. Comparison of indicator kriging, conditional indicator simulation and multiple-point statistics used to model slate deposits. Eng. Geol. 98 (1–2), 50–59.

Bengtsson, M., Gustafson, G., 1996. *Bedömning av grundvatten utgående från grundvatten miljöer* [Publication B426, Gothenburg, Institution of Geology]. Chalmers University of Technology.

Bredehoeft, J., 2005. The conceptualization model problem—surprise. Hydrogeol. J. 13, 37–46. https://doi.org/10.1007/s10040-004-0430-5.

Cashman, P.M., Preene, M., 2001. Groundwater Lowering in Construction: A Practical Guide. CRC Press.

Chen, J., Zhu, B., Wei, Z., 2020. Analysis on Water-Inrush the Process of Deep Excavation in Karst Area Caused by Soil Internal erosion. IOP Conference Series: Earth and Environmental Science.

Claesson, A., 2022. Paleo-Environmental Reconstruction Using a Long Sediment Core from Liseberg, Gothenburg in South-Western Part of Sweden (Publication Number MAR704). University of Gothenburg, Gothenburg.

de Vries, L.M., Carrera, J., Falivene, O., Gratacós, O., Slooten, L.J., 2009. Application of multiple point geostatistics to non-stationary images. Math. Geosci. 41, 29–42.

Enemark, T., Peeters, L.J., Mallants, D., Batelaan, O., 2019. Hydrogeological conceptual model building and testing: a review. J. Hydrol. 569, 310–329.

Enemark, T., Madsen, R.B., Sonnenborg, T.O., Andersen, L.T., Sandersen, P.B., Kidmose, J., Møller, I., Hansen, T.M., Jensen, K.H., Høyer, A.-S., 2024. Incorporating interpretation uncertainties from deterministic 3D hydrostratigraphic models in groundwater models. Hydrol. Earth Syst. Sci. 28 (3), 505–523. https://doi.org/10.5194/hess-28-505-2024.

Fetter Jr., C., 2001. Applied Hydrogeology Fetter Fourth Edition.

Freeze, R.A., James, B., Massmann, J., Sperling, T., Smith, L., 1992. Hydrogeological decision analysis: 4. The concept of data worth and its use in the development of site investigation strategies. Groundwater 30 (4), 574–588.

Haaf, E., Wikby, P., Abed, A., Sundell, J., McGivney, E., Rosén, L., Karstunen, M., 2024. A metamodel for estimating time-dependent groundwater-induced subsidence at large scales. Eng. Geol. 341, 107705.

Haaf, E., Ericsson, L.O., Sundell, J., Liljedahl, L.C., Selroos, J.-O., 2025. Some insights from modeling groundwater levels in open boreholes in crystalline rock in tunneling projects. In: Tunnelling into a Sustainable Future – Methods and Technologies. CRC Press. https://doi.org/10.1201/9781003559047-475.

Hsiung, B.-C.B., 2018. Geohazard caused by groundwater in urban underground excavation. Geofluids 2018 (1), 5820938. https://doi.org/10.1155/2018/5820938.

Hu, L., Chugunova, T., 2008. Multiple-point geostatistics for modeling subsurface heterogeneity: a comprehensive review. Water Resour. Res. 44 (11).

Jørgensen, F., Møller, R.R., Sandersen, P.B., Nebel, L., 2010. 3-D geological modelling of the Egebjerg area, Denmark, based on hydrogeophysical data. GEUS Bull. 20, 27–30.

Kessler, T.C., Comunian, A., Oriani, F., Renard, P., Nilsson, B., Klint, K.E., Bjerg, P.L., 2013. Modeling fine-scale geological heterogeneity—examples of sand lenses in tills. Groundwater 51 (5), 692–705.

Knudby, C., Carrera, J., 2005. On the relationship between indicators of geostatistical, flow and transport connectivity. Adv. Water Resour. 28 (4), 405–421.

Lagerlund, E., Housmark-Nielsen, M., 1993. Timing and pattern of the last deglaciation in the Kattegat region, Southwest Scandinavia. Boreas 22 (4), 337–347.

Langford, J., Baardvik, G., Karlsrud, K., 2016. Pore pressure reduction and settlements induced by deep supported excavations in soft clay. In: Proceedings of the 17th Nordic Geotechnical Meeting.

Li, M.-G., Chen, J.-J., Xia, X.-H., Zhang, Y.-Q., Wang, D.-F., 2020. Statistical and hydro-mechanical coupling analyses on groundwater drawdown and soil deformation caused by dewatering in a multi-aquifer-aquitard system. J. Hydrol. 589, 125365. https://doi.org/10.1016/j.jhydrol.2020.125365.

Li, M.-G., Chen, J.-J., Xu, Y.-S., Tong, D.-G., Cao, W.-W., Shi, Y.-J., 2021. Effects of groundwater exploitation and recharge on land subsidence and infrastructure settlement patterns in Shanghai. Eng. Geol. 282, 105995. https://doi.org/10.1016/j.enggeo.2021.105995.

Li, D., Ma, J., Wang, C., Gao, X., Fang, M., 2022. A new method for piping risk evaluation on unconfined aquifers under dewatering of deep foundation pits. KSCE J. Civ. Eng. 26 (8), 3275–3286.

Lidmar-Bergström, K., 1995. Relief and saprolites through time on the Baltic Shield. Geomorphology 12 (1), 45–61. https://doi.org/10.1016/0169-555X(94)00076-4.

Lissel, P., 2016. Bilaga 2 PM Numerisk grundvattenberäkning Haga. Korsvägen och Almedal, Trafikverket.

Lithén, J., Wadsten, M., Holm Östergaard, S., 2016. PM Hydrogeologi jord. Underlagsdokument till PM Hydrogeologi, ansökan om tillstånd enligt miljöbalken för anläggandet av Västlänken och Olskroken planskildhet. Trafikverket.

Liu, Y., 2006. Using the Snesim program for multiple-point statistical simulation. Comput. Geosci. 32 (10), 1544–1563.

Liu, L.-L., Wang, Y., 2022. Quantification of stratigraphic boundary uncertainty from limited boreholes and its effect on slope stability analysis. Eng. Geol. 306, 106770. https://doi.org/10.1016/j.enggeo.2022.106770.

Liu, N.-W., Peng, C.-X., Li, M.-G., Chen, J.-J., 2022. Hydro-mechanical behavior of a deep excavation with dewatering and recharge in soft deposits. Eng. Geol. 307, 106780. https://doi.org/10.1016/j.enggeo.2022.106780.

Liu, S., Sun, W., Zhang, W., Wang, Y., Liu, Z., Li, Z., Yang, Y., He, Q., Wu, Z., Xiao, P., 2024. Investigation on parameters affecting reduction coefficient of groundwater buoyancy in clay layers. J. Hydrol. 638, 131560.

Lundqvist, J., 1983. Till and moraines in Sweden. In: Ehlers, J. (Ed.), Glacial Deposits in North-West Europe. Balkema, pp. 83–90.

Merisalu, J., Sundell, J., Rosén, L., 2023. Probabilistic cost-benefit analysis for mitigating hydrogeological risks in underground construction. Tunn. Undergr. Space Technol. 131, 104815.

Migoń, P., Lidmar-Bergström, K., 2001. Weathering mantles and their significance for geomorphological evolution of central and northern Europe since the Mesozoic. Earth Sci. Rev. 56 (1–4), 285–324. https://doi.org/10.1016/S0012-8252(01)00068-X.

Miller, U., Robertsson, A., 1988. Late Weichselian and Holocene environmental changes in Bohuslän, southwestern Sweden. Geogr. Pol. 55, 103–111.

Mok, C.M., Carrera, B., Hort, H., Santi, L., Daus, A., Panday, S., Jones, D., Partington, B., Ferguson, E., 2024. Simulation-optimization approach for siting injection wells in urban area with complex hydrogeology. Groundwater 62 (2), 236–249. https://doi.org/10.1111/gwat.13317.

Niswonger, R.G., Panday, S., Ibaraki, M., 2011. MODFLOW-NWT, a Newton formulation for MODFLOW-2005. U.S. Geol. Surv. Tech. Methods 6 (A37), 44.

Pujades, E., Vàzquez-Suñé, E., Carrera, J., Jurado, A., 2014. Dewatering of a deep excavation undertaken in a layered soil. Eng. Geol. 178, 15–27. https://doi.org/10.1016/j.enggeo.2014.06.007.

Refsgaard, J.C., Troldborg, L., Henriksen, H.J., Højberg, A.L., Møller, R.R., Nielsen, A.M., 2010. God praksis i hydrologisk modellering. Geological Survey of Denmark and Greenland.

Refsgaard, J.C., Christensen, S., Sonnenborg, T.O., Seifert, D., Højberg, A.L., Troldborg, L., 2012. Review of strategies for handling geological uncertainty in groundwater flow and transport modeling. Adv. Water Resour. 36, 36–50.

Renard, P., 2007. Stochastic hydrogeology: what professionals really need? Groundwater 45 (5), 531–541.

Renard, P., Allard, D., 2013. Connectivity metrics for subsurface flow and transport. Adv. Water Resour. 51, 168–196.

Rizzo, C.B., de Barros, F.P., 2019. Minimum hydraulic resistance uncertainty and the development of a connectivity-based iterative sampling strategy. Water Resour. Res. 55 (7), 5593–5611.

Sandene, T., Langford, J., Kahlström, M., Long, M., Ritter, S., 2024. Database for deep excavations in soft clay with focus on groundwater drainage and installation effects. J. Geotech. Geoenviron. Eng. 150 (11), 04024108.

Stevens, R.L., Hellgren, L.-G., 1990. A generalized lithofacies model for glaciomarine and marine sequences in the Göteborg area, Sweden. Geologiska Föreningen i Stockholm Förhandlingar 112 (2), 89–105.

Strebelle, S., 2002. Conditional simulation of complex geological structures using multiple-point statistics. Math. Geol. 34 (1), 1–21. https://doi.org/10.1023/a:1014009426274.

Strebelle, S.B., Journel, A.G., 2001. Reservoir Modeling Using Multiple-Point Statistics. SPE Annual Technical Conference and Exhibition?

Sun, W., Zhang, W., Han, L., 2023. Determination of groundwater buoyancy reduction coefficient in clay: model tests, numerical simulations and machine learning methods. Underground Space 13, 228–240.

Sundell, J., Rosén, L., Norberg, T., Haaf, E., 2016. A probabilistic approach to soil layer and bedrock-level modeling for risk assessment of groundwater drawdown induced land subsidence. Eng. Geol. 203, 126–139.

Sundell, J., Haaf, E., Norberg, T., Alén, C., Karlsson, M., Rosén, L., 2019a. Risk mapping of groundwater-drawdown-induced land subsidence in heterogeneous soils on large areas. Risk Anal. 39 (1), 105–124.

Sundell, J., Haaf, E., Tornborg, J., Rosén, L., 2019b. Comprehensive risk assessment of groundwater drawdown induced subsidence. Stoch. Env. Res. Risk A. 33 (2), 427–449.

Sundell, J., Norberg, T., Haaf, E., Rosén, L., 2019c. Economic valuation of hydrogeological information when managing groundwater drawdown. Hydrogeol. J. 27, 1111–1130.

Sundkvist, U., 2016. Ansökan om tillstånd enligt miljöbalken för anläggandet av Västlänken och Olskroken planskildhet. PM Hydrogeologi, Trafikverket.

Tabarsa, A., 2017. Numerical simulation of the consolidation in the presence of sand lenses with time-dependent drainage boundaries. Soil Mech. Found. Eng. 53 (6), 385–390.

Terzaghi, K., 1943. Theory of consolidation. Theor. Soil Mech. 265–296.

Troldborg, L., Refsgaard, J.C., Jensen, K.H., Engesgaard, P., 2007. The importance of alternative conceptual models for simulation of concentrations in a multi-aquifer system. Hydrogeol. J. 15, 843–860.

Troldborg, L., Ondracek, M., Koch, J., Jacob, K., Christian, R.J., 2021. Quantifying stratigraphic uncertainty in groundwater modelling for infrastructure design. Hydrogeol. J. 29 (3), 1075–1089. https://doi.org/10.1007/s10040-021-02303-5.

Urciuoli, G., Comegna, L., Pirone, M., Picarelli, L., 2020. The beneficial role of a natural permeable layer in slope stabilization by drainage trenches. Hydrol. Earth Syst. Sci. 24 (4), 1669–1676.

Vilhelmsen, T.N., Auken, E., Christiansen, A.V., Barfod, A.S., Marker, P.A., Bauer-Gottwein, P., 2019. Combining clustering methods with MPS to estimate structural uncertainty for hydrological models. Front. Earth Sci. 7, 181.

Wikby, P., Haaf, E., Abed, A., Rosén, L., Sundell, J., Karstunen, M., 2024. A grid-based methodology for the assessment of time-dependent building damage at large scale. Tunn. Undergr. Space Technol. 149, 105788.

Woodward, S.J., Wöhling, T., Stenger, R., 2016. Uncertainty in the modelling of spatial and temporal patterns of shallow groundwater flow paths: the role of geological and hydrological site information. J. Hydrol. 534, 680–694.

Xiao, T., Zhang, L.-M., Li, X.-Y., Li, D.-Q., 2017. Probabilistic stratification modeling in geotechnical site characterization. ASCE-ASME J. Risk Uncertainty Eng. Syst. Part A: Civ. Eng. 3 (4), 04017019.

Zhu, B., Zhang, J., Zeng, X.-B., 2023. Analysis of internal erosion in granular soil during deep excavation with a Water-Inrush incident in a covered karst area. Tunn. Undergr. Space Technol. 132, 104932.